Energy Analysis and Shadow Modeling of a Rectangular Type Salt Gradient Solar Pond

Alibakhsh Kasaeian[1], Mohamad Aramesh[1],Fathollah Pourfayaz[1]

Dongsheng Wen[2,3]

[1]Faculty of New Science and Technologies, University of Tehran, Tehran, Iran.

[2]School of Chemical and Process Engineering, University of Leeds, Leeds, UK

[3]School of Aeronautic Science and Engineering, Beihang University, Beijing, PR China.

Abstract

In calculating the total solar energy input into a salt gradient solar pond, the current method was incapable for use in long time periods and the calculation was imprecisefor sunny and shaded areas.The existing relations of solar pond energy analysis can be used for momentary calculations but it is very time-consuming forlong time periods. The shading effect inside the pond affects significantly theenergy storage performance of the pond, especially in small ones.To solve the first problem, the mean values of variable parameters during the time periods is proposed in this work and the 'first mean value theorem for definite integrals' is used for deriving the averageof those parameters. For the second problem,a rectangular pond with vertical walls is investigated, and the exact sunny areas in different depths of the pondare calculated at different time conditions. The experimental data of a previously worked paper is used for validation. The energy efficiency of the low convective zone of the experimental pond is

calculated theoretically, and the results show that the theoretical and experimental values are in good agreement with each other. The experimental data and theoretical results for the energy efficiency are 9.68% and 11.38% for January, 17.54% and 18.92% for May and 28.11% and 30.94% for August,respectively. Therefore, the modified relations can be a good reference for predicting a pond performance before its construction.

Keywords: Salt gradient solar pond; Energy analysis; Shadow effect.

1. Introduction

With increasing concerns of carbon emission and global warming, there is an urgent need to developalternative energy sources to replace fossil fuels in the long term[1]. Developing renewable energy technologies,especially solar-based,has received intensive interest in the last a few decades[2, 3]. Among present technologies for various applications of solar energy, salt gradient solar pond is a promising optionfor solar energy storage due to its unique characteristics such as low cost and high capability for long-term energy storage[4-6]. Many studieshave been conductedon the energy analysis of solar pond in different conditions for the purpose of optimization[7], which is briefly reviewed below.

Jafarzade[8] studied the thermal behavior of a small salt gradient solar pond with wall shading effect in 2004.The effect of vertical walls of a square pond on the reduction of the sunny area was included in the model, and theresult reported an overall efficiency of 10% for the pond. In 2006 Karalikick et al. [9] presented an experimental and theoretical investigation of temperature distributions in an insulated solar pond during both daytime and night time. Theoretical temperature distributions were compared withvarious cases, such as inside the pond, underneath the pond and in the side walls.

In 2008 Karakilicik et al.[10] presented an experimental and theoretical investigation of exergyperformance of a solar pond. The exergy efficiencies were less than the energy efficiencies for each zone of the pond due to the exergy destructions in the zones and losses to the surroundings. Bozkurt et al. [11]presented a heat storage performance investigation of an integrated solar pond with a collector system in 2012. It was concluded that to increase thesystem performance, the zone thicknesses, sunny areas of the pond, number of the collectors and salt gradient system should be modified to achieve higher efficiency and stability of the pond.In the same year, Bozkurt et al. [12]compared the performance of an integrated and a nonintegrated solar pond experimentally, and revealed a higherenergy efficiency for the integrated system.

In 2013 Karakilcik et al.[13] presented an experimental investigation of the energy distribution and energy efficiency of a small rectangular solar pond due to shading effect on each zone, and found that the efficiency of the solar pond was decreasedby increasing the shading area.Atiz et al.[14] in 2014 studied the turbidity effect on the exergy performance of solar ponds under various weather conditions and concentrations. The results showed that the exergyefficiency wassignificantly decreased by increasing the turbidities of the zones. In the same year, Bozkurt et al.[15] presented a theoretical analysis for a solar pond at different geometries for the Adiyaman region in Turkey.The energy efficiency of the solar pond was increased by an increase in the size of the pond. In 2015, Bozkurt et al.[16] presented a new performance model to determine the energy storage efficiency of a solar pond.The heat losses of the solar pond were determined by using the Heat 2 software. The experimental and the theoretical heat storage performance of the lower convective zone of the solar pond were determined, and the results showed that the presented model could predict the efficiency of the pond with a good accuracy.In 2015, Bozkurt et al.[17]investigated the effect of the sunny area ratios on the thermal efficiency of a solar pond model. The results showed that with an increase of sunny area ratio, the performance of the solar pond was increased. Another research by Bozkurt et al.[18] in 2015 studied the performance of a magnesium chloride saturated solar pond. The maximum energy and exergy efficiencies werefound to be respectively 27.41% and 26.04% for the heat storage zone in August.

In all previous studies, the existing equations could be used for the momentary time intervals, but a massive amount of calculations was needed to analyze the energy behavior of solar ponds during a specific period. Moreover, in the previous works, the walls` shading effect was either neglected or was not considered precisely. In this study, the energy analysis of solar pondsis modified for the first time, to eliminate the mentioned drawbacks of previously used methods. The average value of variable parameters are implemented in the modified method, which can be used to calculate the pond performance for a much longer period, yet with much less calculations. .In addition, accurate correlations are presented for rectangular ponds to obtain the exact sunny areas inside the pond in different time and locations. The presented energy analysis method shows better accuracy than the former methods in predicting the behavior of a pond.

2. Energy Analysis

In the correlations for calculating the amount of solar energy entering the pond at different pond depths, various parameters are dependent on the sun incident angle. It is very time consuming in considering the changes of this angle during a day and different seasons in order to find the total amount of the entered energy. A simplification of these correlations can lead to less amount of calculations. In next sections, the principles of this study will be described and then modification of the relations will be discussed.

2.1. Principles

The equation that is being used widely to calculate the energy entering the pond in any depth is given by [19, 20]:

$$Q_{solar} = \beta E A_i h(X_i) \quad (1)$$

where$E$ is the total solar energy flux reaching pond surface ($\frac{W}{m^2}$), β is the fraction of the incident solar radiation that enters the pond, A_i is the sunny area of solar pond at the desired depth of X_i (m^2), and $h(X_i)$ is the ratio of the solar energy reaching to that depth. The value of E can be measured during the desired period or can be inquired from meteorological stations.

The parameters of β, A and h are dependent on the incident angle of solar irradiance to the pond. Therefore Eq. (1) can calculate entering energy to the pond only in short periods of time in which the incident angle can be considered as a constant. On the other hand, for rectangular solar ponds, the azimuth angle can also affect the sunny areas inside the pond, as a change in azimuth angle changes the walls shading. In the previous studies, which considered the shading effect, solar pond direction is assumed to be in a way that the azimuth angle become equal to zero and the shading is limited to only one of the walls [13, 17, 21]. By considering the changes in the azimuth angle during the day, this assumption is valid only for short periods of time. In order to solve the mentioned problems, the equations of those three parameters must be modified. In the first case, the equations must be modified to calculate the solar energy entering the pond at different time intervals. For the second case, the equations must be modified so that the exact sunny area of the pond at different depths and time intervals could be calculated.

To calculate the amount of energy entering the pond at any time intervals, Eq. (1) can be written in the integral form as followings:

$$Q_{solar,tot} = \int_{\theta_{i,1}}^{\theta_{i,2}} \beta E A_i h(X_i)\, d\theta_i \tag{2}$$

And by taking out the parameters that are independent of the incident angle from the integral:

$$Q_{solar,tot} = E \int_{\theta_{i,1}}^{\theta_{i,2}} \beta A_i h\, d\theta_i \tag{3}$$

In these equations, E is time dependent, and it is calculated by multiplying solar irradiance, (which is usually given in kW/m^2 or $kJ/hr.m^2$) into the time of calculations. Since the analytical solution of the three parameters in the integral is so complicated, a numerical solution could be a wiser option. On the other hand by considering a mean value for any of the three parameters in the desired period, the value of $Q_{solar,tot}$ in that period can be calculated using the mean values of those parameters. Therefore, in this case, Eq. (1) can be transformed to Eq. (4):

$$Q_{solar} = \bar{\beta} E \bar{A_i} \bar{h}(X_i) \tag{4}$$

where $\bar{\beta}$, $\bar{A_i}$ and $\bar{h}$ are the mean values of β, A_i and h in the specified period,respectively. For the purpose of finding the mean values of these parameters, the method of first mean value theorem for definite integrals can be used. Based on this theorem, the mean value of a function in a particular range of its variable is equal to the area under the function curve divided by length of variable range [22]:

$$\bar{f}(x) = \frac{1}{b-a} \int_a^b f(x)\, dx \tag{5}$$

Based on this method, modified equations of the mentioned parameters are presented in this paper. In the next sections, parameters of β,h and A will be discussed, respectively.

2.2. Modifying β equation

By considering previous studies, the value of β is given by [19, 20]:

$$\beta = 1 - 0.5\left[\frac{\sin^2(\theta_i - \theta_r)}{\sin^2(\theta_i + \theta_r)} + \frac{\tan^2(\theta_i - \theta_r)}{\tan^2(\theta_i + \theta_r)}\right] \tag{6}$$

whereθ_i is the incident angle and θ_r is the refraction angle. According to the complex relation of β, the analytical integration of this parameter needs complicated mathematical processes.To find a relation forthe integration of β parameter, this parameter can be plotted for all possible values of incident angle (0 to 90 degrees), and an equivalent polynomial can be achieved for it, using curve fitting methods. To do the fitting, it is needed to eliminate θ_r, which is a function of θ_i, from Eq. (6). The relation between these two parameters can be written using theSnell's Lawas followings[23]:

$$n_i \sin(\theta_i) = n_r \sin(\theta_r) \tag{7}$$

wheren_i and n_r are refraction indexes of first and second media.Here these media are air and water and their refraction indexes are equal to 1.0000 and 1.3330, respectively. Thus, the relation between the two angles would be as followings:

$$\sin(\theta_r) = \frac{1.0000}{1.3330}\sin(\theta_i) = 0.75\sin(\theta_i) \tag{8}$$

Furthermore:

$$\theta_r = \sin^{-1}(0.75\sin(\theta_i)) \tag{9}$$

Therefore, value of θ_r can be replaced with $\sin^{-1}(0.75\sin(\theta_i))$:

$$\beta = 1 - 0.5\left[\frac{\sin^2(\theta_i - \sin^{-1}(0.75\sin(\theta_i)))}{\sin^2(\theta_i + \sin^{-1}(0.75\sin(\theta_i)))} + \frac{\tan^2(\theta_i - \sin^{-1}(0.75\sin(\theta_i)))}{\tan^2(\theta_i + \sin^{-1}(0.75\sin(\theta_i)))}\right] \tag{10}$$

It must be noted that in common solar ponds, the operating fluidsare water anddifferent solutions of salt and water. Some exceptions may use other fluids, thus, in such cases the value of the refraction angle must be calculated using Eq. (7) and the proper value must be used in further equations. Also this value changes with increase of salt concentration, but this difference is small and can be generally neglected. So it can be assumed that the value of the refraction anglein all the layers of the pond is equal to that of the pure water.

Using Eq. (10), values of β have been plotted based on values of θ_i (in radian), and its curve has been fitted using MATLAB software. Fig. 1 shows the curve fitting results.

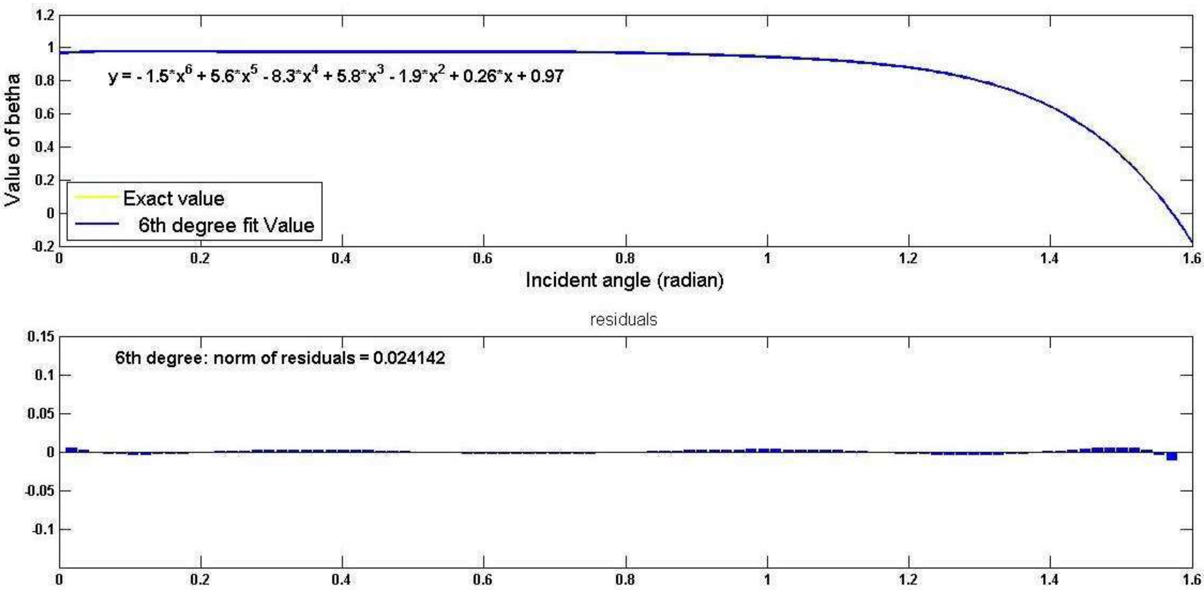

Fig. 1. The difference between values of β_i using the original equation and the fitted equation in all incident angles.

The fitted equation of this parameter, which can calculate the value of β with less than 1% error, is as followings:

$$\beta = -1.5\theta_i^6 + 5.6\theta_i^5 - 8.3\theta_i^4 + 5.8\theta_i^3 - 1.9\theta_i^2 + 0.26\theta_i + 0.97 \tag{11}$$

whereθ_i is in radian form. Hence, the integral of this parameter can be calculated using following equation:

$$\int \beta\, d\theta_i = -\frac{3}{14}\theta_i^7 + \frac{14}{15}\theta_i^6 - \frac{88}{50}\theta_i^5 + \frac{29}{20}\theta_i^4 - \frac{19}{30}\theta_i^3 + 0.13\theta_i^2 + 0.97\theta_i + C \tag{12}$$

The parameter of C is the integral constant and value of it is not a concern in definite integrals. Therefore, the mean value of β can be calculated using Eqs. (5) and (12). It must be noted that according to the definition of the incident angle, if this angle reaches to zero in the desired interval, the mean value must be calculated using the equation below:

$$\bar{\beta} = \frac{\int_0^{\theta_{i,1}} \beta\, d\theta_i + \int_0^{\theta_{i,2}} \beta\, d\theta_i}{(\theta_{i,1} - 0) + (\theta_{i,2} - 0)} \tag{13}$$

2.3. Modifying h equation

Value of h can be calculated by Eq. (14)[19, 20]:

$$h_i = 0.36 - 0.08\, ln\left[\frac{X_i}{cos(\theta_r)}\right] \tag{14}$$

whereX_i is the desired depth (m). Considering theSnell's Law and the logarithm function characteristics:

$$h_i = 0.36 - 0.08[ln(X_i) - ln(cos(sin^{-1}(0.75\,sin(\theta_i))))]$$
$$= 0.36 - 0.08\,ln(X_i) + 0.08[ln(cos(sin^{-1}(0.75\,sin(\theta_i))))] \quad (15)$$

Eq. (15) calculates the value of h as a function of the incident angle. Analytical integration of this equation results in complex numbers. Likewise, the parameter of β, integral of this parameter can be calculated using curve fitting methods. It must be noted that the second term in the right-hand side ($-0.08\ln(X_i)$) is not a function of the incident angle. Thus, for every depths, this parameter can be considered as a constant value. Using MATLAB software and Eq. (15), the fitted equation of$h_i - (-0.08\ln(X_i))$is as followings:

$$h_i + 0.08\,ln(X_i) = 0.0104\theta_i{}^4 - 0.0156\theta_i{}^3 - 0.0132\theta_i{}^2 - 0.0019\theta_i + 0.3601 \quad (16)$$

Then, the relation of h can be written as Eq. (17):

$$h_i = 0.0104\theta_i{}^4 - 0.0156\theta_i{}^3 - 0.0132\theta_i{}^2 - 0.0019\theta_i + 0.3601 - 0.08\,ln(X_i) \quad (17)$$

Fig. 2 shows the accuracy of Eq. (16) for calculating the value of $h_i - (-0.056\ln(X_i))$.

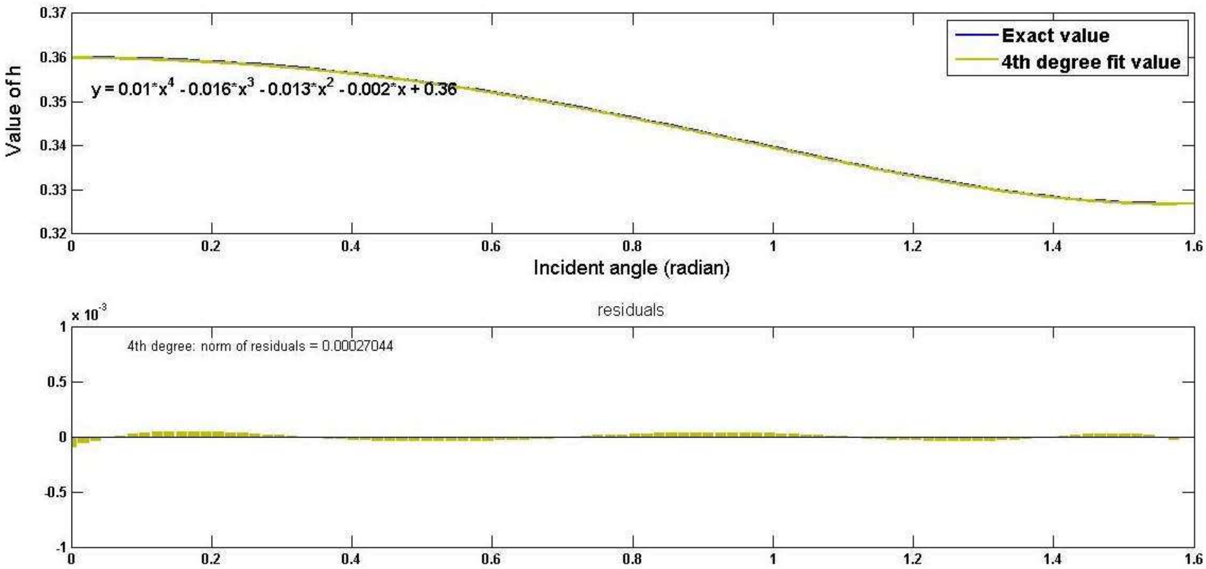

Fig. 2. The difference between values of $h_i + 0.08\ln(X_i)$ using the original equation and the fitted equation in all incident angles.

Eq. (17) is the result of adding the same constant value to both sides of Eq. (16). Therefore, the accuracy of Eq. (17) is the same with Eq. (16) and theerror percentage for calculating the h parameterusing Eq. (17) will be less than 0.02%. In the fitting processes for both parameters of β and h, the incident angle was taken in the radian form, so this parameter in the polynomial equations must be used in the radian form too. Also, the values of the incident angle have been shown in the radian form in Figs. 1 and 2. Integration of Eq. (17) results in the following equation:

$$\int h\,d\theta_i = 0.00200\theta_i^{\,5} - 0.00400\theta_i^{\,4} - 0.00430\theta_i^{\,3} - 0.00100\theta_i^{\,2} + (0.0400 - 0.08\,ln(X_i))\theta_i + C \qquad (18)$$

Similar to Eq. (12), it is not needed to calculate the integral constant in Eq. (18). Therefore, the mean value of h can be calculated using Eqs. (5) and (18). As it was mentioned before, if there is zero incident angle in the interval, the mean value of h can be calculated as followings:

$$\bar{h} = \frac{\int_0^{\theta_{i,1}} h\,d\theta_i + \int_0^{\theta_{i,2}} h\,d\theta_i}{\left(\theta_{i,1} - 0\right) + \left(\theta_{i,2} - 0\right)} \qquad (19)$$

2.4. Calculating exact sunny areas

The sunny area of the pond influencesthe solar energy absorbance [17]. By taking into account the shading of the pond walls, this area is less than the pond cross section. Therefore, to increase the accuracy of the calculations, the shading effect must be studied. In this study rectangular ponds with vertical walls have been investigated. In this type of ponds, the azimuth angle is effective on the walls shading as well as the incident angle. Thus in the next sections firstly the incident and azimuth angles will be discussed and then the proper relations for calculating the sunny areas for this type of ponds will be presented.

- *Solar angles*

In previous studies on the rectangular ponds, only one of the pond's walls were considered to be effective on the shading [8, 13, 17, 21]. This situation would occur only in a short periods because the direction of the solar incident to the pond will vary with the changes in the azimuth angle during the day and various shaded areas will be expected. Thus, to calculate the sunny areas, the effects of the bothincident and azimuth angles must be considered. These angles are dependent on time and location. The value of the incident angle can be calculated using Eq. (20)[23]:

$$\cos(\theta) = \sin(\delta)\sin(\phi)\cos(\beta) - \sin(\delta)\cos(\phi)\sin(\beta)\cos(\gamma) + \cos(\delta)\cos(\phi)\cos(\beta)\cos(\omega) + \cos(\delta)\sin(\phi)\sin(\beta)\cos(\gamma)\cos(\omega) + \cos(\delta)\sin(\beta)\sin(\gamma)\sin(\omega) \quad (20)$$

whereδ is the declination angle, ϕ is the latitude, β is the tilt angle of the pond's surface, γ is the surface azimuth angle and ω is the hour angle. Solar ponds are not tilted, and their surface is horizontal, so the tilt angle is equal to zero. Therefore, the incident angle can be calculated using the equation below:

$$cos(\theta) = sin(\delta)\, sin(\phi) + cos(\delta)\, cos(\phi)\, cos(\omega) \quad (21)$$

The solar azimuth angle for horizontal surfaces can be found using the following equation [23]:

$$\gamma_S = sign(\omega)\left|cos^{-1}\left(\frac{cos(\theta)\,sin(\phi) - sin(\delta)}{sin(\theta)\,cos(\phi)}\right)\right| \tag{22}$$

where$sign(\omega)$ is the sign function of the hour angle. Fig. 3 schematically describes β, γ_S, θ and γ angles.

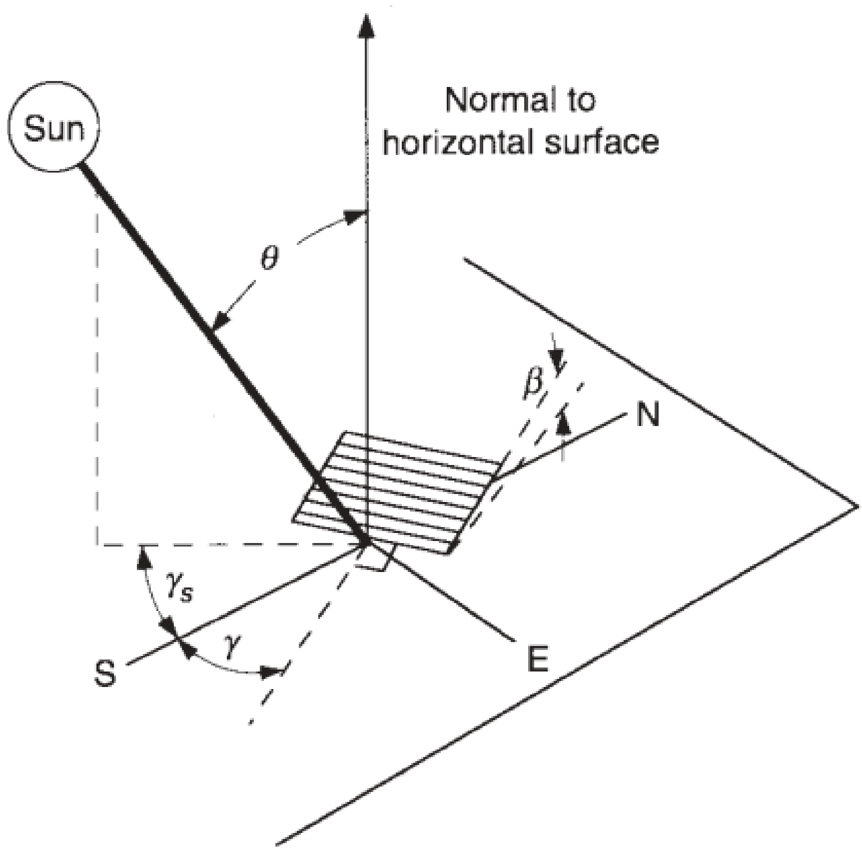

Fig. 3. Schematics of the tilt, surface's azimuth, solar azimuth and incident angles[23]

Here it has been assumed that one of the pond walls is facing to the south, so based on Fig. 3, only the solar azimuth angle effects on shadow creation. In other circumstances, the summation of the solar and surface azimuth angles must be used for calculations.

As it can be seen in Eqs. (21) and (22), the effective angles on the incident and azimuth angles are ϕ, δ and ω. The ϕ angle that represents the latitude, can be determined by the location of the pond. The other two angles can be calculated by their relations. Eq. (23) shows the relation for the declination angle[24]:

$$\delta = 23.44\, sin\left(360\frac{n-80}{365.25}\right) \tag{23}$$

where$n$ is the day number and for the latitudes below 66.5 degrees, this parameter can be defined using Table 1. [25]:

Table 1. Number of days in a year

Month	**Date**	**Day number**
January	1^{st}	1
February	1^{st}	32
March	1^{st}	60
April	1^{st}	91
May	1^{st}	121
June	1^{st}	152
July	1^{st}	181

August	1st	213
September	1st	244
October	1st	274
November	1st	305
December	1st	335

Also, the hour angle can be calculated using following equation[24]:

$$\omega = \frac{360}{86400}(t - 43200) \tag{24}$$

where$t$ is the local solar time in seconds. To calculate solar local time the equation below can be used [23]:

$$t - standard\ time = 4(L_{st} - L_{loc}) + E \tag{25}$$

where standard time is equal to the clock time in the standard local meridian of the pond's location, L_{st} is the standard local meridian longitude, $L_{loc}$is the longitude of the pond's location, and E is the equation of time. It should be mentioned that all the time units in Eq. (25) are in minutes. To use the value of t in Eq. (24), conversion to the second unit must be considered. The value of E in minutes can be calculated using Eq. (26) [24].

$$E = -0.017188 - 0.42811\,cos(B) + 7.35141\,sin(B) \tag{26}$$

where B is the representation of the day number in angle and is defined as followings[24]:

$$B = \frac{360}{365} n \tag{27}$$

Therefore through Eqs. (23) to (27) and considering the latitude of pond's location, the incident angle can be calculated by Eq. (21), and the solar azimuth angle can be foundusing Eq. (22).

The azimuth angle determines the shape of the shadow and incident angle specifiesits size. This is shown schematically in Fig. 4.

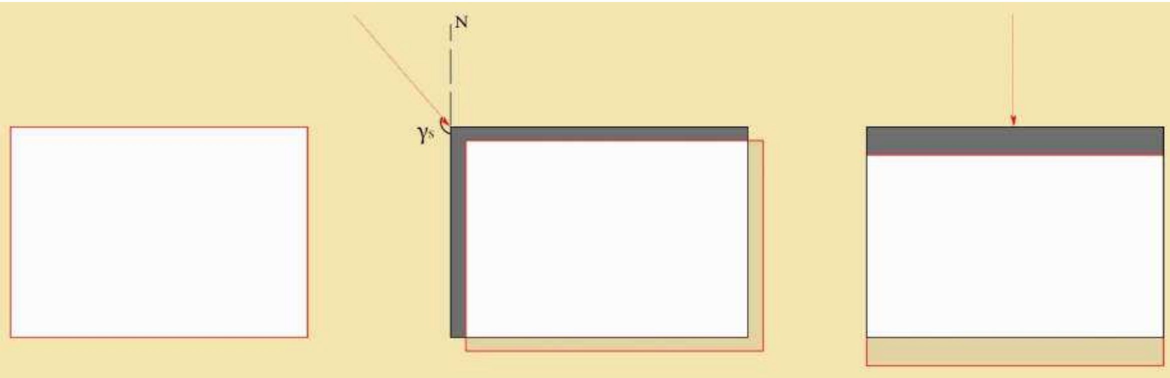

Fig. 4. Effect of the azimuth angle on the shape of the shadow

In this figure, the red rectangle represents the solar radiation area, and the black rectangle represents the solar pond's cross section. The gray surfaces are shaded areas, and the white surfaces are the sunny areas. Hypothetical solar radiation area moves towards left or right by the changes in the value of azimuth angle.It can be concluded from Eqs. (21) to (27) that both incident and azimuth angles are functions of time. Therefore to calculate sunny areas inside the pond, calculations must be performed during the desired period. This can be considered for other parts of this paper since incident angle was introduced as a reference for former calculations while incident angle itself is a function of time.

By defining the basics, calculation of sunny areas in the ponds with rectangular cross sections will be discussed in the next section.

- *Solar ponds with rectangular cross section and vertical walls*

To find sunny areas in these types of ponds, trigonometric and geometric relations must be considered. Fig. 5 reveals the relations between the created shadow and azimuth and incident angles. It must be noted that the refraction angles of azimuth and incident angles cause creating the shadow and the refraction angles will be used in calculations. Also, the size of the shadow inside the pond in different depths is only affected by incident refraction angle. Moreover, azimuth refraction angle just determines the shape of the shadow.

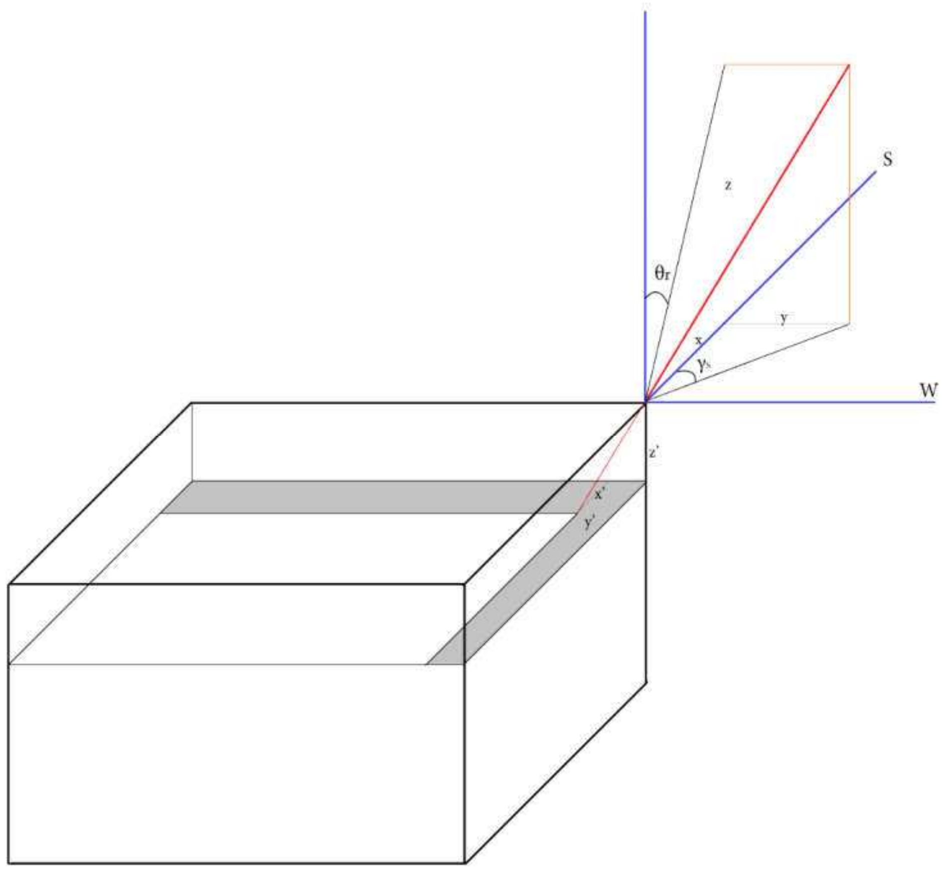

Fig. 5. Effects of azimuth angle on shape of the shadow

In Fig. 5, coordinate axes which represent geographical orientations are shown with blue color, sunlight beam is shown by red color, sunny area in the depth of z' is demonstrated by white color and shadow area in that depth is indicated by gray color. Considering geometric relations, ratios of x, y and z, which form solar radiation vector, remain constant and can be described as followings:

$$\frac{x}{y} = \frac{x'}{y'}, \frac{x}{z} = \frac{x'}{z'}, \frac{y}{z} = \frac{y'}{z'} \tag{28}$$

Therefore for any desired depth such as z', x and y can be calculated considering solar radiation vector components. The ratios between these components are dependent to the refraction angles of incident and azimuth angles:

$$tan\,\theta_r = \frac{x}{z} = \frac{x'}{z'} \quad \Rightarrow \quad x' = z'\,tan\,\theta_r \tag{29}$$

$$tan\,\gamma_s = \frac{y}{x} = \frac{y'}{x'} \quad \Rightarrow \quad y' = x'\,tan\,\gamma_s \quad \Rightarrow \quad y' = z'\,tan\,\theta_r\,tan\,\gamma_s \tag{30}$$

Using Eqs. (29) and (30), for any given depth of the pond, shadow thickness can be determined in x and y directions respectively. To calculate the sunny area, the shadow area must be subtracted from the cross section of the pond. Considering L as length of the pond (north to south direction) and W as width of the pond (east to west direction), due to Fig. 5, following equation, can be written:

$$A = (L \times W) - \left[\left((L - x')y'\right) + \left((W - y')x'\right) + (x' \times y')\right] \tag{31}$$

$$= LW - (Ly' + Wx' - x'y') = LW + x'y' - Ly' - Wx'$$

Using Eqs. (29) and (30), Eq. (31) can be rewritten as followings:

$$A = LW + tan\,\gamma_s\,(z'\,tan\,\theta_r)^2 - Lz'\,tan\,\theta_r\,tan\,\gamma_s - Wz'\,tan\,\theta_r \tag{32}$$

This parameter is a function of incident refraction angle and depth of the pond. Hence, it needs two averaging steps to find the mean value in the desired layer and in desired time interval. According to the complicated relations of this parameter, numerical methods are proper ways for calculation of the mean values.

Thereupon calculation of sunny areas, as well as other parameters in energy relations, were discussed. Using mean values of these parameters in Eq. (4), the solar energy entering the pond can be calculated precisely which will be discussed in next section.

3. Results and Discussion

In this section, before investigating the modified relations, the shading effect will be studied. To do so, dimensions of an experimental salt gradient solar pond constructed in Adiyaman, Turkey, have been considered [17, 21, 26]. The dimensions are mentioned in Table 2.

Table 2. Characteristics of the experimental pond [17, 21, 26].

Pond's depth	**Pond's length**	**Pond's width**	**UCZ thickness**	**NCZ thickness**	**LCZ thickness**
1.5 m	2 m	2 m	0.1 m	0.6 m	0.8 m

Also, four different location and time condition combinations have been assumed which are shown in Table 3.

Table 3. Location and time conditions

Condition	**City (latitude)**	**Day's number-Date (Declination angle)**	**Time (hour angle)**	**Refraction angle**	**Azimuth angle**
Con. 1	Tehran (+35.6961º)	217-August 6th (16.57º)	8 (-60º)	56.2479º	-47.2507º
Con. 2	Tehran (+35.6961º)	217-August 6th (16.57º)	12 (0º)	19.1261º	-2.7046º
Con. 3	Tehran (+35.6961º)	35-feburary 4th (-16.39º)	8 (-60º)	76.3317º	-32.8441º

Con. 4	Singapore (+1.3000°)	217-August 6^{th} (16.57°)	8 (-60°)	69.9493°	39.9614°

Figs. 6 to 8 show the shaded and sunny areas inside the pond in three different depths, for the pond mentioned in Table 2 and the conditions shown in Table 3. The depths are 0.1 m, 0.7 m and 1.5 m which are respectively the intersection between upper convective zone and non-convective zone, the intersection between non-convective zone and lower convective zone and bottom of the pond. In these figures red color represents the sunny areas of the pond and blue color represents shaded areas.

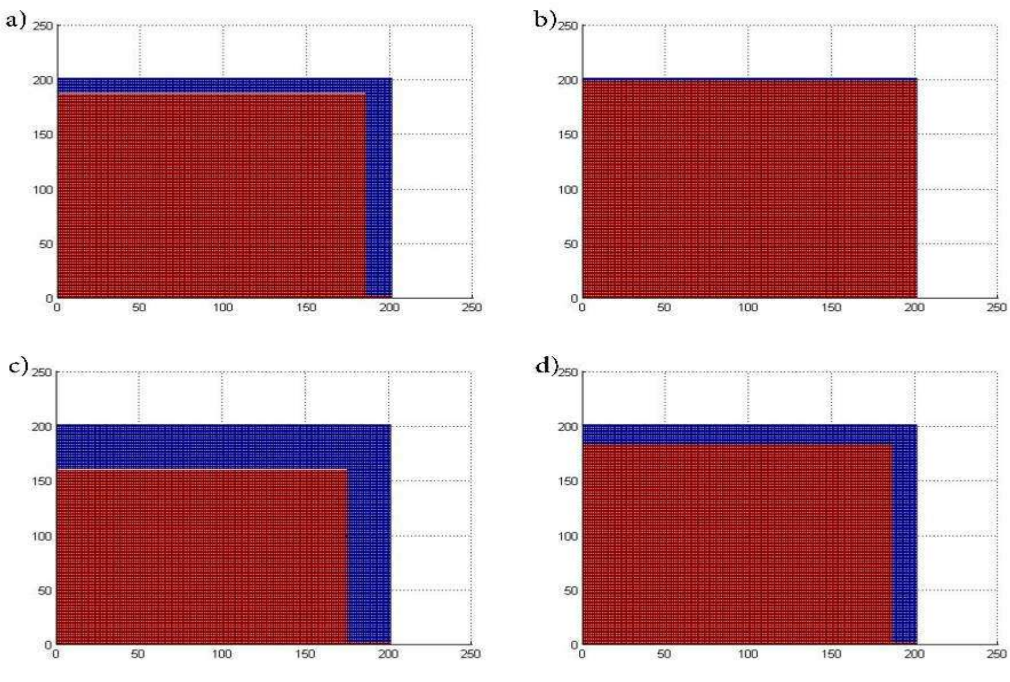

Fig. 6. Sunny and shaded areas at 0.1m depth, for a) Con. 1, b) Con. 2, c) Con. 3 and d) Con. 4

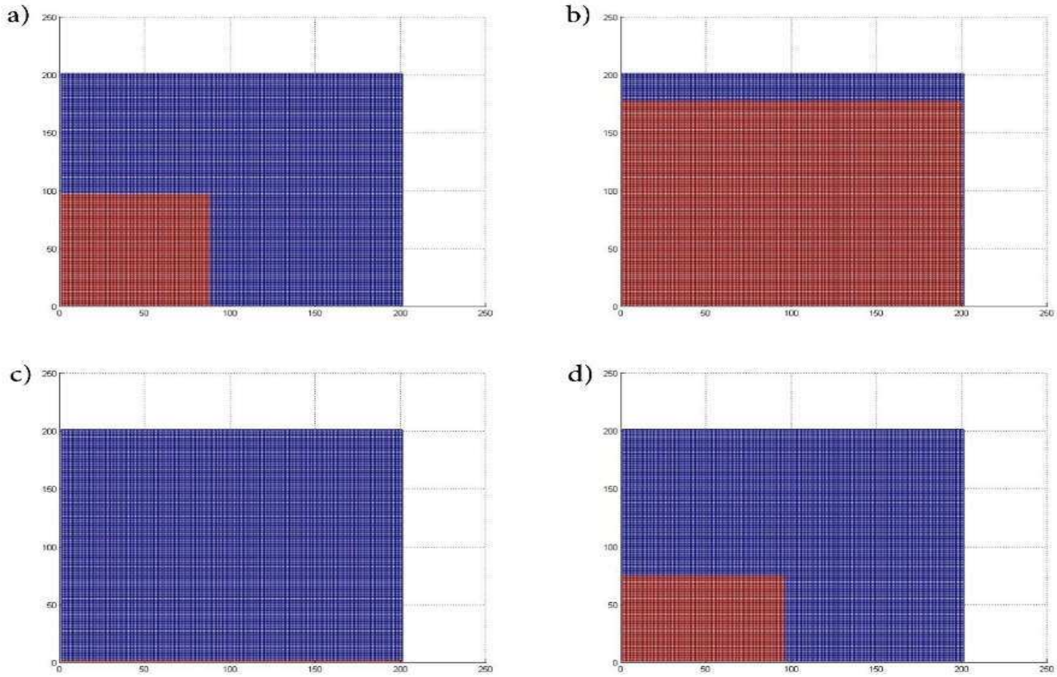

Fig. 7. Sunny and shaded areas at 0.7m depth, for a) Con. 1, b) Con. 2, c) Con. 3 and d) Con. 4

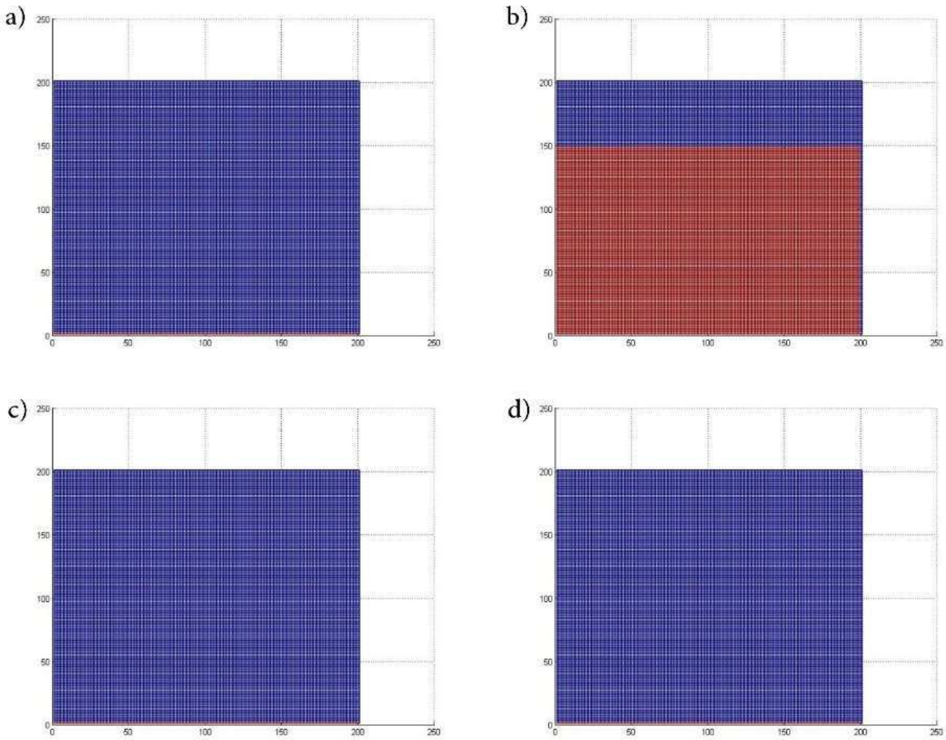

Fig. 8. Sunny and shaded areas at 1.5m depth, for a) Con. 1, b) Con. 2, c) Con. 3 and d) Con. 4

Figs. 6 to 8 show that the shadow created inside the pond can have a significant effect on the energy absorbed inside the pond. For a better understanding of shadow effects, the sunny areas of each case in all of the considered conditions have been calculated and are presented in terms of sunny volume ratios in Table 4. These ratios show the sunny volume of the pond to its total volume.

Table 4. Sunny volume ratios of the pond in all considered cases and conditions

Parameter	Con. 1	Con. 2	Con. 3	Con. 4
Sunny area volume	0.3285	0.6013	0.2987	0.7213

According to the direct effect of sunny areas in energy relations, these values show that neglecting the shading effect can lead to high errors in calculations.

In the next part of results, the accuracy of modified equations will be studied. For this purpose, one of the previous experimental studies on solar pond energy analysis will be considered as a reference. Karaklick et al.(2006) presented an experimental study on a salt gradient solar pond in the city of Adiyaman in Turkey. Experimental data of this pond are given in three different studies [17, 21, 26]. Dimensions of the pond have been mentioned in Table 2, and the energy-related data are shown in Table 5.

Table 5. Experimental data for heat stored in LCZ layer and solar irradiance

parameter	August	May	January
$Q_{stored.LCZ}$ (MJ)	252.65	160.31	18.7
E (MJ/m^2)	690	713	175

The LCZ layer efficiency has been calculated using following equation [26]:

$$\eta_{LCZ} = \frac{Q_{stored.LCZ}}{Q_{solar,LCZ}} \quad (33)$$

where η_{LCZ} is the thermal efficiency of LCZ layer, $Q_{stored.LCZ}$ is the amount of energy which is stored in LCZ layer and $Q_{solar,LCZ}$ is the amount of solar radiation heat which enters this layer and can be calculated using modified relations in this article. Using those relations and experimental data, the energy efficiency of LCZ layer has been calculated theoretically. The theoretical and experimental results are shown in Table 6.

Table 6. Comparison of theoretical and experimental energy efficiencies of LCZ layer

Month	Experimental efficiency [17]	Theoretical efficiency
January	9.68%	11.38%
May	17.54%	18.92%
August	28.11%	30.94%

These results are shown graphically in Fig. 9.

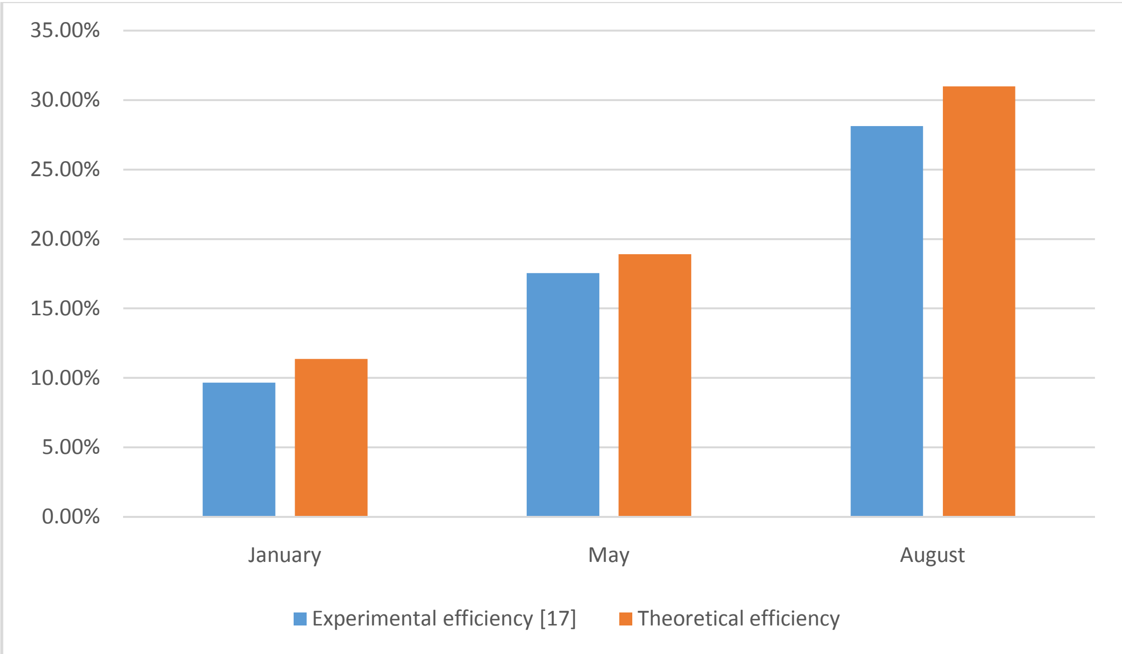

Fig. 9. Graphical comparison of theoretical and experimental energy efficiencies of LCZ layer

The results reported inTable 6 and Fig. 9 show that the theoretical efficiencies are in good agreement with the experimental values. Therefore, this method can predict the values of energy entering the pond or energy efficiencies of different layers with a good accuracy.

4. Conclusion

In this paper, a modified modelingmethod for calculating solar energy entering a salt gradient solar pond and its layers was presented. In the former studies there are two primary limitations:

1. Existing parameters in equations are dependent on the solar incident angle, which varies with time, and the relations can calculate energies only in short periods of time.

2. The shading effectinside the pound, which has a significant impact on the value of energy entering the pond, wasneglected or calculated insufficiently.

The present study deals with the first issue by using mean values of the parameters during the considered time interval. The expressions for parameters of β (i.e., the fraction of solar radiation which enters the pond) and h (i.e., the fraction of total solar energy which reaches to desired depth) were presented. Then, to deal with the second issue, rectangular solar ponds with vertical walls were considered, and proper equations for calculating exact values for sunny areas were presented.

The results from modified equations were compared with a published experimental study and good agreement was found. . The theoretically predicted efficiencies for LCZ layer had 1.7%, 1.38% and 2.83% differences with experimental data for the months of January, May and August respectively. Therefore, this method can be used to predict the amount of energy entering the pond or energy efficiency for different layers of it with a good accuracy. For practical applications,these governing parameters can be easily calculated before building a specified solar pond and the dimensions of it can be optimized to reach a designed outcome.

Refrences

[1] A.M.K. Vandani, M. Bidi, F. Ahmadi, Exergy analysis and evolutionary optimization of boiler blowdown heat recovery in steam power plants, Energy Conversion and Management, 106 (2015) 1-9.

[2] A. Sakhrieh, A. Al-Salaymeh, Experimental and numerical investigations of salt gradient solar pond under Jordanian climate conditions, Energy Conversion and Management, 65 (2013) 725-728.

[3] R. Boudhiaf, M. Baccar, Transient hydrodynamic, heat and mass transfer in a salinity gradient solar pond: A numerical study, Energy Conversion and Management, 79 (2014) 568-580.

[4] Z. Hongfei, J. Hua, Z. Lianying, W. Yuyuan, Mathematical model of the thermal utilization coefficient of salt gradient solar ponds, Energy Conversion and Management, 43 (2002) 2009-2017.

[5] M. Husain, P.S. Patil, S.R. Patil, S.K. Samdarshi, Combined effect of bottom reflectivity and water turbidity on steady state thermal efficiency of salt gradient solar pond, Energy Conversion and Management, 45 (2004) 73-81.
[6] H. Kurt, F. Halici, A.K. Binark, Solar pond conception — experimental and theoretical studies, Energy Conversion and Management, 41 (2000) 939-951.
[7] M. Husain, S.R. Patil, P.S. Patil, S.K. Samdarshi, Simple methods for estimation of radiation flux in solar ponds, Energy Conversion and Management, 45 (2004) 303-314.
[8] M.R. Jaefarzadeh, Thermal behavior of a small salinity-gradient solar pond with wall shading effect, Solar Energy, 77 (2004) 281-290.
[9] M. Karakilcik, K. Kıymaç, I. Dincer, Experimental and theoretical temperature distributions in a solar pond, International Journal of Heat and Mass Transfer, 49 (2006) 825-835.
[10] M. Karakilcik, I. Dincer, Exergetic performance analysis of a solar pond, International Journal of Thermal Sciences, 47 (2008) 93-102.
[11] I. Bozkurt, M. Karakilcik, The daily performance of a solar pond integrated with solar collectors, Solar Energy, 86 (2012) 1611-1620.
[12] I. Bozkurt, M. Karakilcik, I. Dincer, Energy efficiency assessment of integrated and nonintegrated solar ponds, International Journal of Low-Carbon Technologies, 9 (2012) 45-51.
[13] M. Karakilcik, I. Dincer, I. Bozkurt, A. Atiz, Performance assessment of a solar pond with and without shading effect, Energy Conversion and Management, 65 (2013) 98-107.
[14] A. Atiz, I. Bozkurt, M. Karakilcik, I. Dincer, Investigation of turbidity effect on exergetic performance of solar ponds, Energy Conversion and Management, 87 (2014) 351-358.
[15] I. Bozkurt, A. Atiz, M. Karakilcik, I. Dincer, Performance Analysis of a Solar Pond, in: I. Dincer, A. Midilli, H. Kucuk (Eds.) Progress in Exergy, Energy, and the Environment, Springer International Publishing, Cham, 2014, pp. 783-790.
[16] I. Bozkurt, S. Mantar, M. Karakilcik, A new performance model to determine energy storage efficiencies of a solar pond, Heat Mass Transfer, 51 (2015) 39-48.
[17] I. Bozkurt, M. Karakilcik, The effect of sunny area ratios on the thermal performance of solar ponds, Energy Conversion and Management, 91 (2015) 323-332.
[18] I. Bozkurt, S. Deniz, M. Karakilcik, I. Dincer, Performance assessment of a magnesium chloride saturated solar pond, Renewable Energy, 78 (2015) 35-41.
[19] I. Bozkurt, Reply to "Erroneous equations used to assess the performance of a solar pond" by Morteza Khalilian, Energy Conversion and Management, 114 (2016) 399.
[20] M. Khalilian, Erroneous equations used to assess the performance of a solar pond, Energy Conversion and Management, 114 (2016) 394-398.
[21] I. Dincer, M.A. Rosen, EXERGY: Energy, Environment and Sustainable Development, Elsevier Science, 2012.
[22] R.C. James, G. James, The Mathematics Dictionary, Springer Netherlands, 1992.
[23] W.A.B. John A. Duffie, Solar Engineering of Thermal Processes, 4th Edition, New York, 2013.
[24] A.V. da Rosa, Fundamentals of Renewable Energy Processes (Third Edition), Academic Press, Boston, 2012.
[25] S.A. Klein, Calculation of monthly average insolation on tilted surfaces, Solar Energy, 19 (1977) 325-329.
[26] M. Karakilcik, I. Dincer, M.A. Rosen, Performance investigation of a solar pond, Applied Thermal Engineering, 26 (2006) 727-735.